Visualizing the Spin of Individual Cobalt-Phthalocyanine Molecules

C. Iacovita,[1] M. V. Rastei,[1] B. W. Heinrich,[1] T. Brumme,[2] J. Kortus,[2] L. Limot,[1,*] and J. P. Bucher[1]

[1]*Institut de Physique et Chimie des Matériaux de Strasbourg UMR 7504, Université Louis Pasteur, F-67034 Strasbourg, France*

[2]*Institut für Theoretische Physik, TU Bergakademie Freiberg, D-09599 Freiberg, Germany*

(Received 5 May 2008; published 12 September 2008)

Low-temperature spin-polarized scanning tunneling microscopy is employed to study spin transport across single cobalt-phthalocyanine molecules adsorbed on well-characterized magnetic nanoleads. A spin-polarized electronic resonance is identified over the center of the molecule and exploited to spatially resolve stationary spin states. These states reflect two molecular spin orientations and, as established by density functional calculations, originate from a ferromagnetic molecule-lead exchange interaction.

DOI: 10.1103/PhysRevLett.101.116602 PACS numbers: 72.25.−b, 73.20.At, 75.70.Rf, 85.65.+h

Conceptually new device structures accounting for sizable quantum effects will be needed if the downscaling of electronic and magnetic devices is to continue. One of these new concepts consists in merging molecular electronics and spintronics, so that functional molecules become active device components within a circuitry where information is carried by electronic spins [1,2]. Progress toward this tantalizing goal relies on our understanding of spin transport and magnetism in reduced dimensions, where fundamental playgrounds extend to the extreme limit of single atoms and molecules. Studies include spin transport across a well-chosen molecule attached to two magnetic leads [3,4], or even atomic-size constrictions formed by bringing two magnetic leads into contact [5,6]. The variability of the resulting conductance due to the incomplete control over the molecule-lead interface has attracted little experimental interest so far [7,8]. A better understanding of this limiting drawback would allow us to engineer the desired spintronic functionalities into a molecule.

In recent years it has become possible with spin-polarized (SP) scanning tunneling microscopy and spectroscopy (STM and STS) to probe spin-polarized tunnel transport over selected areas of a surface, or even single objects, with atomic-scale resolution. In this way, for example, the current-driven rotation of a nanocluster's magnetization was shown to depend on the spatial location of the spin injection [9]. It was also shown that some control could be exerted on spin transport through an atom deposited on a magnetic surface by a careful choice of the atomic element [10].

In this Letter we demonstrate that tunneling spin transport is possible through an atom "dressed" with organic ligands. We combine low-temperature SP-STM and model calculations to study a reference system consisting of individual cobalt-phthalocyanine [CoPc, Fig. 1(a)] molecules adsorbed on a magnetic substrate. The interaction between the molecule and the substrate results in two molecular spin orientations, which are clearly discernible in the differential conductance (dI/dV) of the SP tunnel junction. Our results provide a direct visualization of stationary spin states that differ from the molecular Kondo state where spin flips occur in time [11–15]. As demonstrated here, this is a consequence of the ferromagnetic coupling between the molecular spin and the magnetic substrate.

The measurements were performed in a STM operating below 10^{-10} mbar at a temperature of 4.6 K. After cleaning the Cu(111) single crystal by repeated cycles of Ar^+ sputtering and annealing to 500 °C, the surface was cooled to room temperature and cobalt was subsequently deposited onto it by *e*-beam evaporation. This leads, at submonolayer coverage, to the formation of triangularlike nanoislands two-atomic layers high [Fig. 1(b)]. Cobalt islands were chosen since they are a well-studied system [16–18], with, at low temperature, a magnetization perpen-

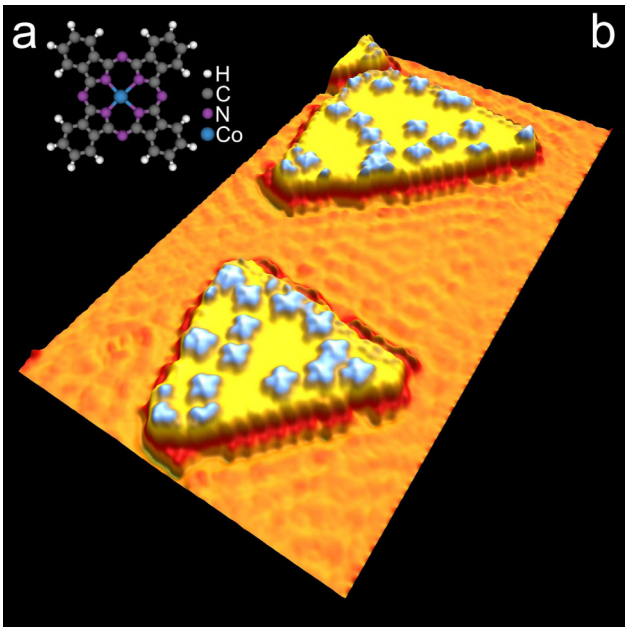

FIG. 1 (color online). CoPc molecules adsorbed on cobalt nanoislands grown on Cu(111). (a) Structure model for CoPc. (b) Pseudo-three-dimensional STM image (40×20 nm^2, 0.1 V, 0.5 nA). The spatial oscillations on the Cu(111) surface are due to the scattering of the Shockley surface-state electrons.

dicular to the surface with a "up" or "down" orientation. Finally CoPc was sublimated onto the sample by heating to at least 400 °C a crucible containing a 99.5% pure CoPc powder. Low-temperature constant-current images showed that CoPc adsorbs preferentially on cobalt, either on top of the nanoislands or along their step edges [Fig. 1(b)]. All sample preparations repeatedly showed this preferential adsorption. Typical island coverage was roughly 10 molecules for an area of $(10\ \mathrm{nm})^2$. On the islands, CoPc exhibits a four-lobe pattern 1.4 nm wide consistent with the ideal structure of the molecule.

Co-coated metal tips were employed because we found that they posses an out-of-plane component of the magnetization parallel to the island magnetization. The spin-dependent contribution to the dI/dV varies in fact with $\cos\alpha$, where α is the angle between the magnetization of the tip and of the sample [19]. The dI/dV versus sample bias (V) was recorded by superimposing a sinusoidal modulation to the junction bias of amplitude 5 mV rms at a frequency of 7 kHz, and detecting the first-harmonic of the current through a lock-in amplifier. The dI/dV in the center of the islands in the absence of CoPc are marked by a dominant SP resonance falling at -0.28 V below the Fermi energy [Fig. 2(a)], which is believed to arise from the hybridization of s-p states with the minority $d_{3z^2-r^2}$ band of the island [18]. The amplitude of the resonance is sensitive to the spin polarization of the Co islands, so that islands with opposite magnetization can be discerned through single-point spectroscopy or through a contrast in spectroscopic maps [see Fig. 3(b) where $V = -0.29$ V]. In the following, islands presenting a strong dI/dV signal at -0.28 V are designated as parallel (noted ⇈), while the remaining as antiparallel (⇅). This designation is arbitrary (at -0.60 V the dI/dV intensities are reversed with respect to -0.28 V) and does not refer to the relative alignment of the tip and islands magnetizations. All the spectra presented were recorded over islands of *hcp* stacking with lateral dimensions larger than 12 nm. This ensures that the spectroscopic contrast is purely spin polarized, since the electronic contrast related to stacking [17] or size-dependent relaxations [18] is then constant over the investigated islands.

Spin-polarized spectra of CoPc were acquired by positioning the tip over the Co atom of CoPc [Fig. 2(b)]. A broad resonance centered at -0.19 V is detected for all CoPc molecules residing on ⇈ islands, whereas a resonance of weaker amplitude is found for molecules on ⇅ islands, indicating that the cobalt atom is spin polarized. Here after, CoPc molecules are noted ⇈ if residing on parallel islands, and ⇅ if residing on antiparallel islands. If this proves that the CoPc and island magnetizations are linked, their alignment as well as the nature of the magnetic coupling between CoPc and the island remain unknown. Nevertheless, this shows that the molecular magnetization may be switched by inverting the island magnetization, for example, using an external magnetic field [17]. This result is particularly appealing in view of spin-dependent molecular electronics as suggested recently by a study on ultrathin films of metalloporphyrin [8]. While the resonance is fairly reproducible, the structure at lower biases was found to be tip dependent [Fig. 2(b)]. To get a clearer picture, we have plotted the asymmetries of both CoPc and the cobalt islands [Fig. 2(c)] averaged over 13 different tips. The asymmetry is defined as $(⇈ - ⇅)/(⇈ + ⇅)$, the arrows referring to a dI/dV acquired on ⇈ and ⇅ CoPc molecules or islands, respectively. An oscillatory behavior is observed with a sign reversal occurring at -0.26 and

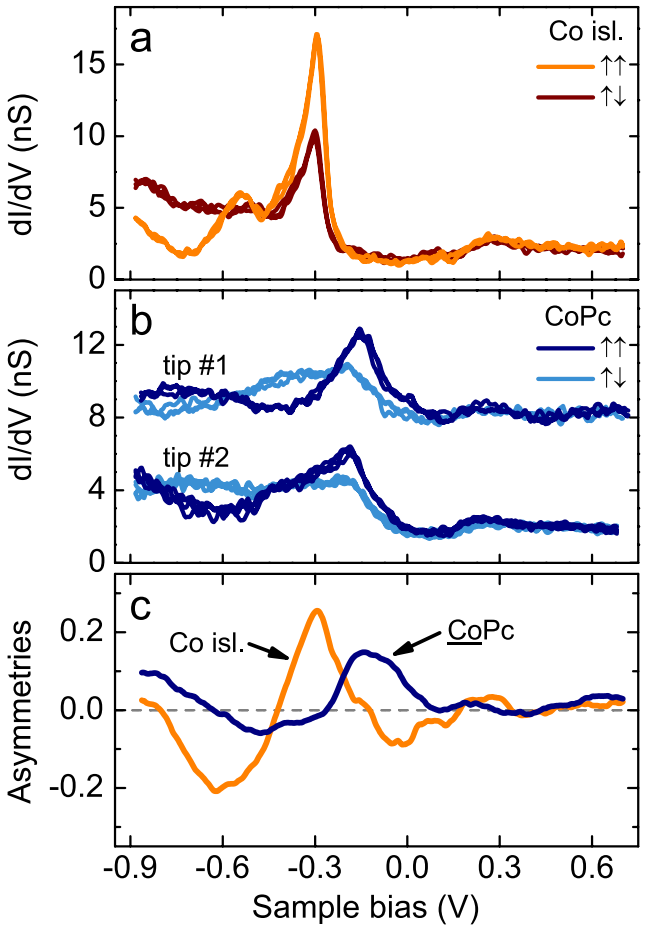

FIG. 2 (color online). Spin-polarized tunneling conductance through the nanoislands and CoPc. (a) Typical spin-polarized dI/dV over two cobalt nanoislands of opposite magnetization (noted ⇈ and ⇅). Feedback loop opened at 0.6 V and 0.5 nA. (b) Differential conductance (dI/dV) over the center of single CoPc molecules adsorbed on cobalt nanoislands of opposite magnetization. Two sets of spectra acquired with distinct tips (noted 1 and 2) are presented. The spectra acquired with tip 1 are displaced upward by 6 nS for clarity. Feedback loop opened at 0.6 V and 0.5 nA. (c) Asymmetries arising from opposite magnetizations for CoPc and the Co nanoislands. The asymmetries are an average of all the recorded asymmetries obtained with different tips.

−0.64 V for CoPc, and at −0.12, −0.42, and −0.80 V for the islands.

A visual rendering of the dI/dV spectra is presented in Fig. 3, where the pixel intensity on each image corresponds to the differential conductance at a given sample bias. These images, or dI/dV maps, show isolated CoPc molecules on two islands of opposite contrast. A marked island contrast (areas without CoPc) is visible in Fig. 3(a) since the bias is then −0.29 V, which corresponds to a high magnetic asymmetry [see Fig. 2(c)]. The right island is ↑↑, whereas the left one is ↑↓. A similar contrast is observed in the absence of CoPc [Fig. 3(b)]. On the contrary, CoPc molecules have similar intensities on both islands, as expected by the molecular asymmetry which is close to zero at this bias. A contrast between ↑↑ and ↑↓ molecules becomes visible when moving upward or downward in energy, as one may expect from the behavior of the asymmetry depicted in Fig. 2(c). While the islands have nearly the same intensity at −0.16 V [Fig. 3(c)], the CoPc asymmetry is now maximal. The molecules appear as round dots, with a higher intensity for CoPc molecules residing on the ↑↑ island compared to CoPc on the ↑↓ island [Fig. 3(d)]. A contrast is also detected at −0.32 V [Fig. 3(e)], but is now reversed compared to the previous map. The benzene ring of the organic ligand [Fig. 3(f)] appears dim while a bright area 1 nm wide is centered at the Co atom. We observed that the SP signal, when present,

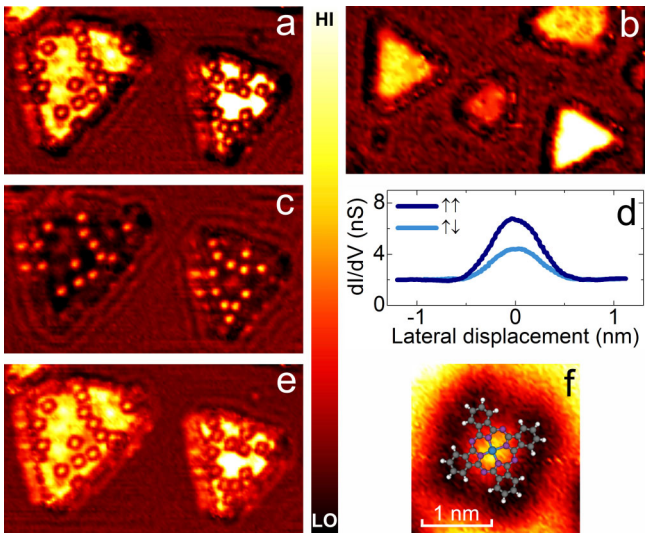

FIG. 3 (color online). Spin-polarized tunneling conductance maps for CoPc. Maps (a), (c), and (e) were taken at −0.29, −0.16, and −0.32 V, respectively (image size: 40 × 20 nm^2). Each map is normalized to span the same color palette range. Feedback loop opened at 0.6 V and 0.5 nA. (b) Spin-polarized map of Co nanoislands at −0.29 V—as in (a)—in the absence of CoPc molecules (45 × 25 nm^2). (d) Profiles of the differential conductance along one axis of CoPc extracted from (c). Molecules on the ↑↑ island [right island in (c)] have the highest profile. (f) Map of a ↑↓ molecule of (e) with model molecular structure superimposed (2.6 × 2.6 nm^2).

is spatially limited to this area (see also Fig. S1 in the auxiliary information [20]).

To gain insight into the twofold spin orientation of CoPc observed by SP-STM, we first focus on the nature of the magnetic coupling between CoPc and the island, and then tentatively provide a link to the data by calculating the differential conductance. As a starting point, we determine the adsorption geometry of CoPc through first-principles calculations based on density functional theory by means of the PWSCF package [21]. The magnetic surface is mimicked by using a slab model consisting of three Cu layers with two Co layers on top and about 2.2 nm vacuum to the next periodic repeated layer. The CoPc was placed above the Co layers resulting in a 302 atom model. During the geometry optimization, only the Cu atoms where held fixed at their positions according to bulk values, whereas CoPc and the two Co layers where allowed to fully relax. Different starting geometries with the cobalt atom of CoPc in a top, bridge, and hollow position have been checked. The lowest energy from the geometry optimization has been obtained for the bridge position [Fig. 4(a)]. The calculated distance between the surface atoms and the cobalt atom of CoPc is about 0.25 nm, close to the Co-Co distance in the surface layers, with a surface distortion of only 0.02 nm or lower occurring (Fig. S2 of [20]). Based on the partial density of states (PDOS) [Fig. 4(b)], an hybridization between Co surface atoms and N (C) atoms at binding energies between −4 to −5 eV provides the chemical bonding of the molecule to the surface. Figure 4(b) also shows that an hybridization between the molecular Co and N exists, as can be recognized from the occurrence of peaks close in energy below −4 eV for the $3d$ states of Co and $2p$ states of N. In particular, compared to the free CoPc molecule where the d_{z^2} state is unoccupied, it is here broadened over several electronvolts below E_F, resulting in a reduced magnetic moment of $0.7\mu_B$.

The magnetization density [Fig. 4(c)] shows a clear ferromagnetic coupling between CoPc and the surface. While the largest magnetization density is found close to the cobalt atoms, as expected, there is also a magnetization of $0.05\mu_B$ or lower at some nitrogen and carbon atoms pointing in the opposite direction with respect to the cobalt atoms. This small magnetization might explain the absence of a SP signal over these atoms. The bridge position is driven by the interaction of the four N atoms around the central cobalt atom of CoPc [Fig. 4(a) here and Fig. S2 of [20]]. The angles between the Co surface atom, the N atom on top, and the cobalt atom from CoPc are close to 90°, favoring then a ferromagnetic exchange according to the Goodenough-Kanamori rules for superexchange [22]. This indirect exchange coupling mechanism is in accordance with the conclusions drawn for metalloporphyrins [8]. Here, however, the direct Co-CoPc distance is comparable to the average distance within the cobalt surface and direct exchange contributes as well.

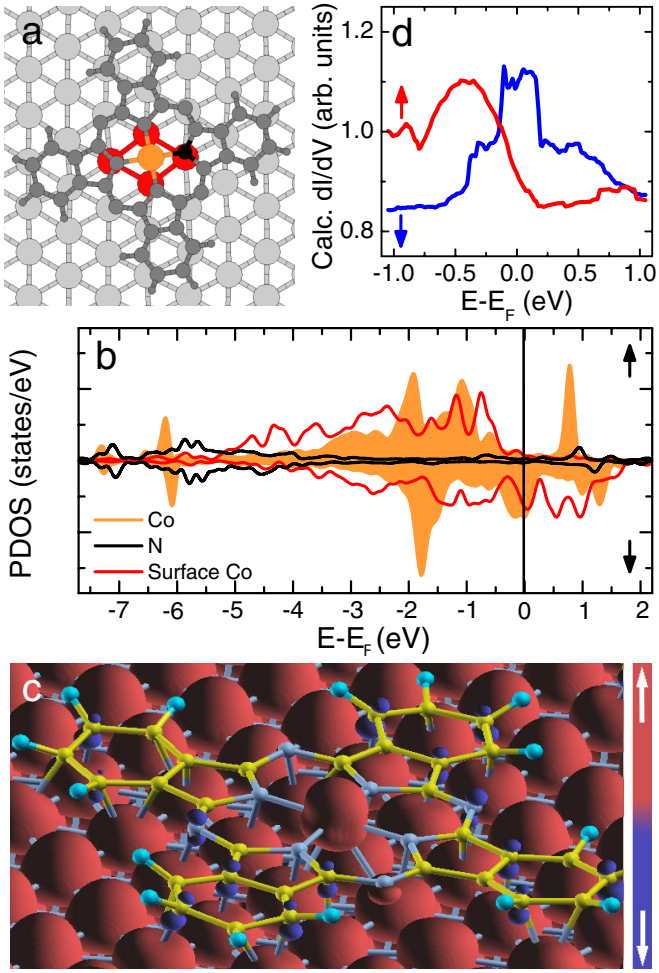

FIG. 4 (color online). Electronic and magnetic structure of CoPc on the cobalt nanoislands. (a) Schematic adsorption geometry of CoPc. (b) PDOS over CoPc and the cobalt surface (top panel, majority PDOS; bottom panel, minority PDOS). (c) Isosurface plot of the magnetization density ($\uparrow$, magnetization in the "up" direction; $\downarrow$, "down" direction). The cobalt atom of CoPc and the cobalt atoms of the surface have parallel magnetizations. (d) Calculated differential conductance based on [19] (majority, $\uparrow$; minority, $\downarrow$).

Finally, to link our calculations to the experimental dI/dV curves we exploit the spin-dependent charge densities over the cobalt atom of CoPc according to the Tersoff-Hamann approximation [23], and perform a numerical derivative with respect to energy assuming a parallel alignment of tip and sample magnetization. This approach gives the same results as the more straightforward method outlined in Ref. [19]. The dI/dV curves near E_F for majority and minority states [noted $\uparrow$ and $\downarrow$, respectively, in Fig. 4(d)] are dominated by contributions from cobalt d states of CoPc, namely, d_{xz}, d_{yz}, and d_{z^2} states. Although encouraging similarities are found with the SP-STS data of Fig. 2(b), a change of contrast being even predicted at -0.15 eV, detailed transport calculations including spin-orbit coupling are required to improve the agreement.

With the ultimate lateral resolution of SP-STM we have shown that the spin state of a single molecule can be directly visualized by means of spin-polarized tunnel electrons. A ferromagnetic interaction, partly carried by the organic ligands, is predicted between CoPc and the surface. The ligands also play an important role in the adsorption geometry of CoPc. This may hint to the possibility of influencing spin transport through ligand modification.

This work was supported by the European Union Network of Excellence MAGMANet (FP6-515767-2) and the Agence Nationale de la Recherche (ANR-07-BLAN-0139). We would like to thank the ZIH Dresden for providing computational resources and assistance.

*limot@ipcms.u-strasbg.fr

[1] A. R. Rocha *et al.*, Nature Mater. **4**, 335 (2005).
[2] L. Bogani and W. Wernsdorfer, Nature Mater. **7**, 179 (2008).
[3] K. Tsukagoshi, B. W. Alphenaar, and H. Ago, Nature (London) **401**, 572 (1999).
[4] J. R. Petta, S. K. Slater, and D. C. Ralph, Phys. Rev. Lett. **93**, 136601 (2004).
[5] H. D. Chopra, M. R. Sullivan, J. N. Armstrong, and S. Z. Hua, Nature Mater. **4**, 832 (2005).
[6] A. Sokolov, C. Zhang, E. Y. Tsymbal, J. Redepenning, and B. Doudin, Nature Nanotech. **2**, 171 (2007).
[7] A. Scheybal *et al.*, Chem. Phys. Lett. **411**, 214 (2005).
[8] H. Wende *et al.*, Nature Mater. **6**, 516 (2007).
[9] S. Krause, L. Berbil-Bautista, G. Herzog, M. Bode, and R. Wiesendanger, Science **317**, 1537 (2007).
[10] Y. Yayon, V. W. Brar, L. Senapati, S. C. Erwin, and M. F. Crommie, Phys. Rev. Lett. **99**, 067202 (2007).
[11] P. Wahl *et al.*, Phys. Rev. Lett. **95**, 166601 (2005).
[12] A. Zhao *et al.*, Science **309**, 1542 (2005).
[13] V. Iancu, A. Deshpande, and S.-W. Hla, Phys. Rev. Lett. **97**, 266603 (2006); Nano Lett. **6**, 820 (2006).
[14] L. Gao *et al.*, Phys. Rev. Lett. **99**, 106402 (2007).
[15] Y.-S. Fu *et al.*, Phys. Rev. Lett. **99**, 256601 (2007).
[16] L. Diekhöner *et al.*, Phys. Rev. Lett. **90**, 236801 (2003).
[17] O. Pietzsch, A. Kubetzka, M. Bode, and R. Wiesendanger, Phys. Rev. Lett. **92**, 057202 (2004).
[18] M. V. Rastei *et al.*, Phys. Rev. Lett. **99**, 246102 (2007).
[19] D. Wortmann, S. Heinze, Ph. Kurz, G. Bihlmayer, and S. Blügel, Phys. Rev. Lett. **86**, 4132 (2001).
[20] See EPAPS Document No. E-PRLTAO-101-059836 for extra experimental and theoretical data supporting the conclusions drawn in our Letter. For more information on EPAPS, see http://www.aip.org/pubservs/epaps.html.
[21] PWSCF is part of the Quantum-ESPRESSO package (www.pwscf.org).
[22] J. B. Goodenough, *Magnetism and the Chemical Bond* (Wiley, New York, 1963).
[23] J. Tersoff and D. R. Hamann, Phys. Rev. Lett. **50**, 1998 (1983).